Journal of Molecular Structure 1056–1057 (2014) 339–346

Contents lists available at ScienceDirect

Journal of Molecular Structure

journal homepage: www.elsevier.com/locate/molstruc

"Push–pull" 1,8-naphthalic anhydride with multiple triphenylamine groups as electron donor

Limin Wang, Yan Shi, Yingyuan Zhao, Heyuan Liu, Xiyou Li *, Ming Bai *

Key Laboratory of Colloid and Interface Chemistry, Ministry of Education, Department of Chemistry, Marine College, Shandong University, Jinan 250100, China

HIGHLIGHTS

- Three new naphthalic anhydride compounds with linear triphenylamino oligomer were prepared.
- The enhanced electron donating ability of the donor leads to excited state changes from ICT state to electron transfer.
- Theoretical calculation reveals that a higher ICT states may responsible for the weak emission of **3**.

ARTICLE INFO

Article history:
Received 1 August 2013
Received in revised form 2 October 2013
Accepted 3 October 2013
Available online 12 October 2013

Keywords:
Push–pull
Absorption spectra
Fluorescence spectra
Triphenylamine
Naphthalic anhydride

ABSTRACT

In this paper, the "push–pull" molecules consisting of different number of triphenylamino groups and 1,8-naphthalic anhydride ring were designed and synthesized. The UV–vis absorption and emission spectra of these compounds were recorded. Along with the increase on the number of the electron donating triphenylamino groups, both the absorption and emission bands show significant red shift. More importantly, the fluorescence quantum yields drop sharply along with the increase on the number of triphenylamino groups. The molecular structure, the frontier molecular orbital energies and the energy gaps between the highest occupied molecular orbital (HOMO) and the lowest un-occupied molecular orbital (LUMO) were calculated with DFT method. The calculated results indicate that the connection of more electron donating triphenylamino groups in molecule caused a change for the first excited state from an intramolecular charge transfer (ICT) state to an intramolecular electron transfer state (ET). This change on the first excited state has led to the fluorescence quenching.

1. Introduction

Due to the unique photophysical properties, 1,8-naphthalimide compounds have found application in various areas of chemistry [1–3]. Moreover, their absorption and emission spectra can be easily tuned through careful structural modification on either the aromatic 'naphthalene' moiety itself, or at the nitrogen of the imide site [4]. Consequently, the 1,8-naphthalimide compounds has been extensively used as strongly absorbing and colorful dyes [5], building block for artificial light harvesting arrays [6], and fluorescent chemical probes [7–9] for the sensing of biologically relevant cations and anions [5,10,13].

The photophysical properties of 1,8-naphthalimide compounds are governed by the nature of the substituent. Connection of electron donating groups at C-4 position of the naphthalic ring give a "push–pull" electronic configuration and generate an intramolecular charge transfer (ICT) excited state [11–13]. This ICT character leads to a large excited-state dipole and broad absorption and emission bands centered at longer wavelength. The ICT transition is highly solvent dependent, and therefore, their photophysical properties, such as the λ_{max} of absorption and emission spectra, the fluorescence quantum yield as well as the fluorescence lifetime, are all dramatically affected by the property of solvents [11,4]. As the most important precursor for 1,8-naphthalimide compounds, 1,8-naphthalic anhydride compound have very similar properties with the corresponding imide compounds. They have the same "push–pull" electronic configuration and similar ICT excited states.

Triphenylamino group is well known for its good electron donating abilities [14]. It has been introduced to the C-4 position of naphthalic ring by Jiang and co-workers for the first time [15]. The electron donating nature of triphenylamino group had induced significant red-shift on the maximum of both absorption and emission. In the present work, we introduced linearly arranged triphenylamino groups as electron donor at the C-4 position of naphthalic ring (**1**–**4** in Scheme 1), which we believe have stronger electron donating ability. The object of this research is to reveal the effects of enforced electron donating ability of the substituents at

* Corresponding authors. Tel.: +86 531 88369877.
E-mail address: xiyouli@sdu.edu.cn (X. Li).

0022-2860/$ - see front matter © 2013 Elsevier B.V. All rights reserved.
http://dx.doi.org/10.1016/j.molstruc.2013.10.004

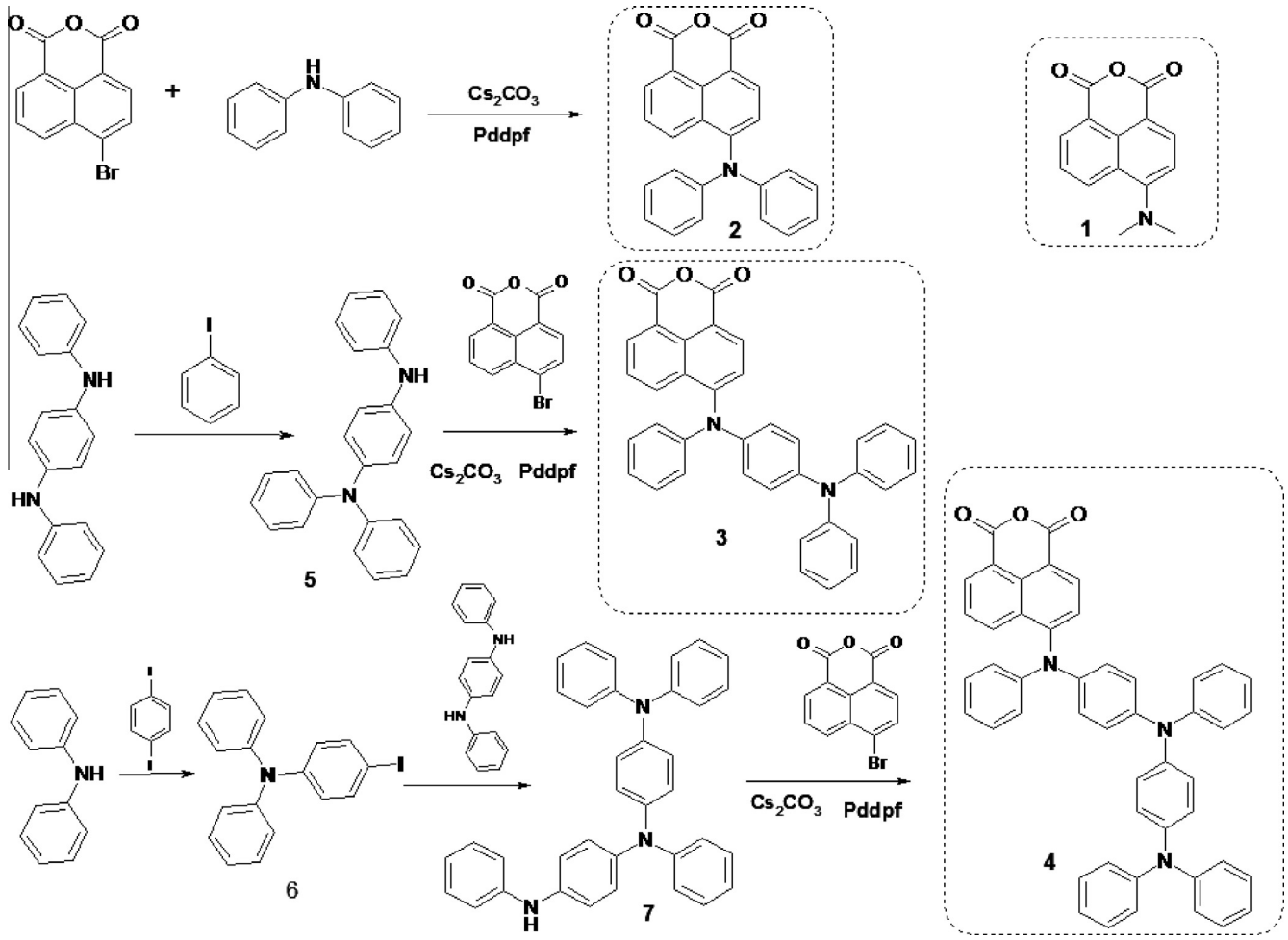

Scheme 1. Molecular structures and synthesis of the title compounds.

C-4 position on the photophysical properties of naphthalic anhydride.

2. Experimental

2.1. General methods

^{1}H NMR and ^{13}C NMR spectra were recorded on a Bruker DPX300 spectrometer (300 MHz) in $CDCl_3$ with TMS as the internal standard (chemical shifts are given as δ in parts per million). ESI-TOF mass spectra were taken on a Q-TOF6510 Angilent instrument. Maldi-TOF mass spectra were taken on a Bruker/ultra flex instrument. The elemental analyses were performed on an Elementar Vario Micro. Electronic absorption spectra were recorded on a Shimadzu UV-2450 spectrophotometer. Steady state fluorescence spectra were recorded on a K2 system of ISS. Electrochemical measurements were carried out under nitrogen atmosphere on an electrochemical working station. The cell comprised inlets for a glassy carbon disk working electrode of 2.0 mm in diameter and a silver-wire counter electrode. The reference electrode was Ag/Ag^+, which was connected to the solution by a Luggin capillary whose tip was placed close to the working electrode. It was corrected for junction potentials by being referenced internally to the ferrocenium/ferrocene (Fe^+/Fe) couple [$E_{1/2}(Fe^+/Fe) = 501$ mV vs. SCE]. Typically, a 0.1 mol dm^{-3} solution of $[Bu_4N][ClO_4]$ in dichloromethane containing 0.5 mmol dm^{-3} of sample was purged with nitrogen for 10 min, then the voltammograms were recorded at ambient temperature. The scan rate was 20 and 10 mV s^{-1} for cyclic voltammetry (CV) and differential pulse voltammetry (DPV), respectively.

2.2. The details of quantum chemical calculation

The hybrid density function B3LYP (Becke–Lee–Young–Parr composite of exchange-correction functional) method [16–18] and the standard 6-31G(d) basis set [19] were used for both structure optimization and the property calculations, which has been proved to be more accurate in simulating vibrational spectra compared with the Hartree–Fock method [20]. No imaginary frequency is predicted, indicating that the optimized structures are true energy-minimums. Based on the energy-minimized structure generated in the last step, charge population calculations were carried out with a full natural bond orbital analysis (NBO) population method [21] and the molecular orbital distribution are discussed according to the NBO results. All the calculations were performed using the Gaussian 03 program [22] in the IBM P690 system at the Shandong Province High Performance Computing Centre.

2.3. Materials and synthesis

N,N′-diphenyl-p-phenylenediamine and diphenylamine were purchased from commercial source and used as received without further purification. Solvents were of analytical grades and were purified by standard methods. The synthetic procedures of the target compounds are outlined in Scheme 1.

*2.3.1. 4-Dimethylamino-1,8-naphthalic anhydride (**1**) [23]*

4-Dimethylamino-1,8-naphthalic anhydride was prepared following the literature methods with a yield of 80% [23]. Mp. 208–210 °C; ^{1}H NMR (300 MHz, $CDCl_3$, 25 °C, TMS): δ 8.59 (d, 1H), 8.51–8.46 (m, 2H), 7.69 (t, 1H), 7.10 (d, 1H), 3.18 (s, 6H); MS(ESI): m/z, calculated for $C_{14}H_{11}O_3N$: 241.25, found: 242.19 [M + H$^+$].

*2.3.2. 4-Diphenylamino-1,8-naphthalene anhydride (**2**)*

To a three-necked flask, 4-bromo-1,8-naphthalic anhydride (276 mg, 1 mmol), diphenylamine (254 mg, 1.5 mmol), [Pd(dppf)Cl_2] (3.65 mg, 0.0050 mmol) and cesium carbonate (488 mg, 1.5 mmol) were added. The flask was purged with nitrogen gas for several times and then 1,4-diethylene dioxide (3 ml) was added via a syringe [29]. The mixture was heated to 95 °C under the protection of nitrogen flow and kept at this temperature for about 3 h. After cooled to room temperature, a mixture of water (3 ml) and ethyl acetate (20 ml) was added to the flask, the organic layer was then separated from the aqueous layer in a separation funnel and washed successively with water and brine solution. The organic layer was dried over anhydrous magnesium sulfate for overnight. After filtration, the solvents were removed under reduced pressure. The residue was purified by column chromatography on silica gel with chloroform/petroleum (v/v = 2/1) as eluent. Compound **2** was collected as orange powder (310.2 mg, 85%). Mp > 300 °C; 1H NMR (300 MHz, $CDCl_3$, 25 °C, TMS): 8.55 (d, 1H), 8.48 (d, 1H), 8.23 (d, 1H), 7.54 (t, 1H), 7.38 (d, 1H), 7.35 (m, 4H), 7.15 (m, 2H), 7.06 (m, 4H). ^{13}C NMR (75 MHz, in $CDCl_3$): 161.00, 160.21, 152.46, 148.15, 134.33, 133.36, 132.82, 132.71, 129.81, 127.59, 126.40, 124.84, 124.47, 124.38, 119.39. MS (ESI): m/z, calculated for $C_{24}H_{15}O_3N$: 365.11, Found: 365.38 [M$^+$]. IR (KBr, cm^{-1}) 1687 (ν^{as} C═O), 1652 (ν^{s} C═O).

*2.3.3. N,N-diphenyl-N′-phenyl-1,4-diaminobenzene (**5**)*

A mixture of N,N′-diphenyl-*p*-phenylenediamine (260 mg, 1 mmol), [Pd(dppf)Cl_2] (3.65 mg, 0.05 mmol), sodium *tert*-butoxide (144 mg, 1.5 mmol), toluene (10 ml) was stirred at 112 °C for 5 min under the protection of nitrogen, iodobenzene (1.2 mmol) was then added to the flask via a syringe. Then the reaction mixture was kept at this temperature for 5 h. After cooled to room temperature, water (3 ml) and ethyl acetate (20 ml) was added to the mixture. The organic layer was separated from the aqueous layer through a separation funnel, and washed successively with water and brine solution. After dried over anhydrous magnesium sulfate for overnight, the solvents were evaporated under reduced pressure. The residue was purified by column chromatography on silica gel with chloroform/petroleum (v/v = 2:1) as eluent. Compound **5** was collected as green powder (210.4 mg, 65%). MS (ESI): m/z, calculated for $C_{24}H_{20}N_2$: 336.43, found: 336.11 [M$^+$]. Elemental analysis (%), calculated for $C_{24}H_{20}N_2$: C 78.60, H 5.94, N 8.32; found: C 78.47, H 6.12, N 8.45.

*2.3.4. 4-(N-phenyl-N-(4-(N′,N′-diphenyl)amino)phenyl)amino-1,8-naphthalene anhydride (**3**)*

Following the similar procedures as that of compound **2**, except with N,N-diphenyl-N′-phenyl-1,4-diaminobenzene (**5**) instead of diphenylamine, compound **3** was obtained as red solid (266.5 mg, 50%). Mp > 300 °C; ^{1}H NMR (300 MHz, $CDCl_3$, 25 °C, TMS): 8.56–8.47 (m, 2H), 8.27 (d, 1H), 7.56–7.50 (t, 1H), 7.40 (d, 1H), 7.31–7.24 (m, 7H), 7.11–6.91 (d, 12H). MS (MALDI-TOF): m/z, calculated for $C_{36}H_{24}O_3N_2$: 532.18, found: 533.19 [M + H]$^+$. Elemental analysis (%) calculated for $C_{36}H_{24}O_3N_2$: C 81.17, H 4.51, N 5.26; found: C 80.63, H 4.72, N 4.72. IR (KBr, cm^{-1}) 1690 (ν^{as} C═O), 1662 (ν^{s} C═O).

*2.3.5. N-(4-iodophenyl)-N-phenyl-benzenamine (**6**)*

To a mixture of 1,4-diiodobenzene (396 mg, 1.2 mmol), diphenylamine (169 mg, 1 mmol), CuI (19 mg, 0.1 mmol), phenanthroline (28.2 mg, 0.12 mmol) and potassium hydroxide (224 mg, 4 mol), dry toluene (20 mL) was added under the protection of nitrogen. Then mixture was heated to 120 °C and kept at this temperature for about 12 h. After then, the reaction was quenched by the addition of water (30 ml). The reaction mixture was extracted with CH_2Cl_2 (30 ml) for three times and the combined organic extracts were dried over anhydrous magnesium sulfate for overnight. Then the organic solvent was evaporated under reduced pressure. The residue was purified by column chromatography on silica gel using petroleum ether as eluent. N-(4-iodophenyl)-N-pheny-benzenamine (**6**) was obtained as a white powder (315.4 mg, 85%). Mp > 300 °C; ^{1}H NMR (300 MHz, $CDCl_3$): 7.58 (d, 2H), 7.28 (m, 4H), 7.08 (m, 6H), 6.83 (d, 2H). MS (ESI): m/z, calculated for $C_{18}H_{14}IN$: 371.21, found: 372.02 [M + H]$^+$.

*2.3.6. N-(4-(N′,N′-diphenyl)amino)phenyl-N-(4-(N‴-phenyl)amino) phenyl-N-phenyl-amine (**7**)*

A mixture of N,N′-diphenyl-*p*-phenylenediamine (260 mg, 1 mmol), N-(4-iodophenyl)-N-phenyl-benzenamine (6445 mg, 1.2 mmol), [Pd(dppf)Cl_2] (3.65 mg, 0.005 mmol), sodium *tert*-butoxide (144 mg, 1.5 mmol) and toluene (10 mL) was stirred at 112 °C for 5 h under the protection of nitrogen. After cooled to room temperature, a mixture of water (3 ml) and ethyl acetate (20 ml) was added to the reaction mixture. The organic layer was separated from the aqueous layer and washed successively with water and brine solution, and dried over anhydrous magnesium sulfate for overnight. Then the solvents were evaporated under reduced pressure. The residue was purified by column chromatography on silica gel with chloroform/petroleum (v/v = 3:1) as eluent. N-(4-(diphenylamino)phenyl)-N,N′-diphenyl-1,4-diaminobenzene (**7**) was collected as dark green powder (251.5 mg, 50%). Mp > 300 °C; ^{1}H NMR (400 MHz, $CDCl_3$): 7.45 (d, 4H), 7.28 (m, 8H), 7.13 (m, 12H), 7.01 (t, 4H). MS (MALDI-TOF): m/z, calculated for $C_{36}H_{29}N_3$: 504.24, found: 503.64 [M$^+$].

*2.3.7. 4-(N-(4-(N′,N′-diphenyl)amino)phenyl-N-(4-(N‴-phenyl)amino)-phenyl-N-phenyl)amine-1,8-naphthalic anhydride (**4**)*

Following similar procedures as that of compound **2**, except with N-(4-(N′,N′-diphenyl)amino)phenyl-N-(4-(N‴-phenyl)amino)phenyl-N-phenyl-amine (**7**) instead of diphenylamine, compound **4** was obtained as red dark solid (210.1 mg, 30%). ^{1}H NMR (400 MHz, $CDCl_3$): 8.54 (m, 2H), 8.27 (d, 1H), 7.54 (t, 1H), 7.34–7.35 (b, 10H), 6.99–7.11 (br, 19H). ^{13}C NMR (75 MHz, in $CDCl_3$): 161.085, 160.225, 148.201, 134.367, 133.326, 132.853, 130.898, 129.735, 129.351, 128.840, 126.153, 125.685, 125.212, 124.141, 123.849, 123.135, 139.397. MS (MALDI-TOF): m/z, calculated for $C_{48}H_{33}O_3N_3$: 699.79, Found: 700.26 [M + H$^+$]. Elemental analysis (%) calculated for $C_{48}H_{33}O_3N_3$: C 82.31, H 4.72, N 6.00; found: C 81.71, H 5.43, N 4.63. IR (KBr, cm^{-1}) 1687 (ν^{as} C═O), 1650 (ν^{s} C═O).

3. Results and discussion

3.1. Synthesis

The introduction of dimethylamine at the C-4 position of 1, 8-naphthalic anhydride has been achieved by heating N,N-dimethyl-2-nitrile-ethylamine in *iso*-propanol following the literature methods [23], which leads to the formation of compound **1**. 4-Bromo-1,8-naphthalic anhydride reacts with diphenylamine in the presence of palladium-catalyst to generate compound **2**. Under similar conditions, compound **3** is obtained by the reaction of

4-bromo-1,8-naphthalic anhydride with N,N-diphenyl-N′-phenyl-1,4-diaminobenzene (**5**) while compound **4** was obtained by the reaction of 4-bromo-1,8-naphthalic anhydride with N-(4-(N′,N′-diphenyl)amino)phenyl-N-(4-(N‴-phenyl)amino)phenyl-N-phenylamine (**6**). The important precursor **5** and **7** were prepared by the palladium-catalyzed reaction of corresponding amines with iodobenzene or N-(4-iodophenyl)-N-phenyl-benzenamine (**6**). Compound **5** gave correct mass spectrum and reasonable elemental analysis results, but failed to give a meaningful ^{1}H NMR. All the signals in ^{1}H NMR spectra are significantly broad and the integrations are unreliable. Because we synthesized compound **3** in a good yield with this product as precursor, we can conclude that the structure of compound **5** is correct.

3.2. Absorption spectra

The absorption spectra of these four compounds in dichloromethane at the concentration of 10^{-5} mol/L are shown in Fig. 1. The corresponding spectrum parameters are summarized in Table 1. As indicated in the absorption spectra, compound **1** shows one absorption peak at 425 nm, which can be assigned to the ICT band [24]. Another band in the UV region, which might be ascribed to the absorption of π–π^* transition of naphthalic ring, cannot be completely shown duo to the limit of instrument. Other three compounds show similar absorption spectra with one ICT band in the visible region and another band around 300 nm in the UV region. The absorption band around 300 nm can be assigned to the absorption of triphenylamino groups of compounds **2**, **3** and **4** [25]. The spectral parameters of compound **2** as shown in Table 1 revealed that the replacement of dimethylamino group with diphenylamino group at C-4 position of naphthalic ring leads to a 38 nm red-shift on the ICT absorption band. This can be attributed to the stronger electron donating ability of diphenylamino group in relative to that of dimethylamino group. When the number of triphenylamino groups in compounds **3** and **4** increased to 2 and 3 respectively, the ICT band further red shifted for about 31 and 9 nm respectively. This result suggests that the increasing on the number of triphenylamino groups has indeed enhanced the electron donating ability of the "push" end of the "push–pull" molecules.

The absorption of triphenylamine subunits at about 300 nm of compounds **2**, **3**, and **4** show some differences. The absorption of the triphenylamine subunit in compound **2** is presented as a small shoulder of the absorption of naphthalic ring in the range of 300–350 nm. But this absorption band became more significant in the absorption spectra of compound **3** due to the doubled number of triphenylamino groups in this molecule. As expected, this absorption band became more significant in the absorption spectra of compound **4** due to the even more triphenylamino groups. More interestingly, the peak of this absorption band appears at about 321 nm, which red shifted for about 9 nm in relative to that of compound **3**. This red-shift suggests the presence of efficient interactions between the triphenylamino groups within both compounds **3** and **4**. This has also been proved by the theoretical calculation as mentioned below.

Table 1
Parameters of absorption and fluorescence spectra of compounds **1**–**4** in dichloromethane.

Compounds	λ, nm ($\varepsilon/10^3$ L mol^{-1} cm^{-1})	Φ (%)[a]
1	~280 (29), 425 (14.7)	100
2	280 (33), 463 (14.4)	5.7
3	312 (49.4), 494 (13.4)	1.0
4	321 (69.2), 503 (13.6)	0

[a] Relative fluorescence quantum yields of these compounds (**2**–**4**: λ_{ex} = 440 nm, **1**: λ_{ex} = 380 nm) calculated with compound **1** as reference.

The absorption spectra of these compounds in different solvents with different polarities are also recorded and the resulted spectra are shown in Supporting Information, Fig. S7. The polarity of the solvent does not show large effects on the absorption spectrum of these compounds on both absorption intensity and absorption wavelength. Only very small red shift on the maximal absorption band of these compounds in polar solvents in relative to that in non-polar solvent can be identified from the spectra. This is because the stabilization of polar solvents to the polar ICT excited states has decreased the energy gap between the ground states and excited states, and consequently leads to the small red-shift on the maximal absorption peak. Because the absorption position determined predominately by the ground states as Frank Condon principle suggested, the solvation of the polar solvents to the ICT excited states does not show large effects on the absorption spectra.

3.3. Fluorescence spectra

The fluorescence spectra of compounds **1**–**3** are shown in Fig. 2. When these compounds were excited by light (380 nm for **1**, 440 nm for **2** and **3**), the ICT emission band was observed. The

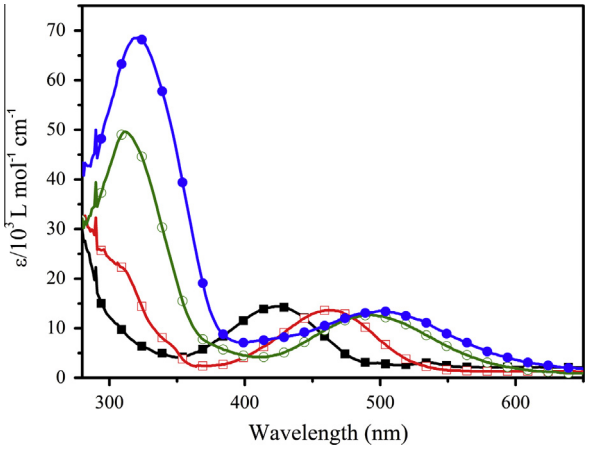

Fig. 1. UV–vis absorption of compound **1** (black line with closed squares), compound **2** (red line with open squares), compound **3** (green line with open circles) and compound **4** (blue line with closed circles) in dichloromethane (10^{-5} mol/L). (For interpretation of the references to color in this figure legend, the reader is referred to the web version of this article.)

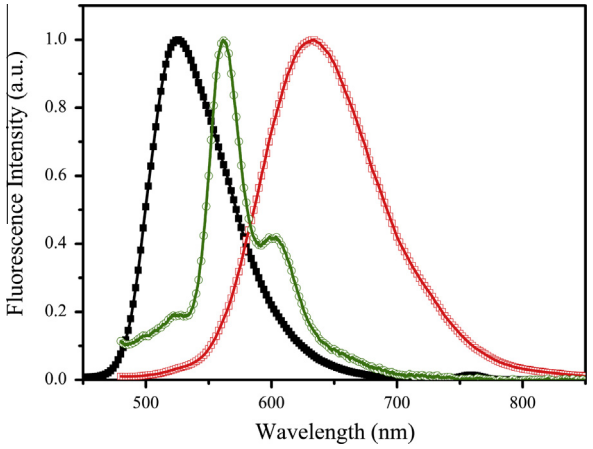

Fig. 2. Normalized fluorescence spectra of compound **1** (black line with closed squares) compound **2** (red line with open squares) compound **3** (green line with open circles) in dichloromethane at concentration 10^{-5} mol/L (**2**–**3**: λ_{ex} = 440 nm, **1**: λ_{ex} = 380 nm). (For interpretation of the references to color in this figure legend, the reader is referred to the web version of this article.)

ICT emission band of compounds **1** and **2** appeared at 526 nm and 633 nm respectively, which is in accordance with the results of absorption spectra. But the ICT emission for compound **3** appeared at 560 nm, which is unexpected because the ICT emission should further red shifted in relative to that of compound **2**. At the very beginning, we suspected that this might be the emission from some impurities, but the excitation spectra as well as the elemental analysis, HPLC analysis reveal the high purity of this compound, therefore, we attribute this emission to a high excited state emission, which will be further discussed lately. Compound **4** did not show any identical ICT emission in the fluorescence spectra. The ICT nature of the fluorescence of compounds **1**–**2** is further proved by their solvent dependent fluorescence spectra, Fig. S8 in Supporting Information. It can be seen that the maximal emission position shifts to red in polar solvent, which is accompanied with distinctive decrease on the fluorescence quantum yield. This can be attributed to the solvation of the polar solvents to the polar ICT excited states, which has reduce the energy of excited states significantly, and then caused the remarkable red-shift of the maximal emission peak.

The fluorescence quantum yields of these four compounds in dichloromethane are measured with compound **1** as reference. The results are summarized in Table 1. It can be found that the fluorescence quantum yield of compound **2** is much smaller than that of compound **1**, which can be attributed to the stronger electron donating ability of diphenylamine than that of dimethylamine [26–29]. The fluorescence quantum yield of compounds **3** and **4** are extremely small, which suggests again that the connection of triphenylamino groups in compounds **3** and **4** has indeed enhanced the electron donating abilities of the group at the C-4 position. This is in line with the results of absorption spectra.

3.4. The electrochemical properties

To investigate the effects of the electron donating groups at the C-4 position on the oxidation and reduction properties of these compounds, the redox potentials were measured by DPV experiments. The results are summarized in Table 2. Compound **1** cannot give any reliable reduction or oxidation signals in both DPV and CV experiments in the electrochemical window of the solvent. The first oxidation of compound **2** happens at 0.93 V and a reduction at −1.35 V. After the introduction of another triphenylamino group, compound **3** shows its first oxidation at 0.51 V, which is much smaller than that of compound **2**. This means the first oxidation of compound **3** happens on the triphenylamino group. Besides the first oxidation, the second oxidation is observed at 0.87 V for compound **3**. The first oxidation potential of compound **4** is further reduced to 0.30 V. Moreover, other two oxidation process are observed at 0.61 and 1.12 V, which correspond to the second and third oxidation, respectively. The difference of the oxidation potentials of compounds **2**–**4** suggests that the first oxidation happens on the triphenylamino groups. More triphenylamino groups are introduced, the easier these molecules are oxidized. Along with the increase on the number of triphenylamino groups, the reduction potentials of compounds **2**–**4** decrease following the order of **2** > **3** > **4**. But the magnitude of the reduction potential decrease is much smaller than that of the first oxidation potentials. This result suggests that the reduction happened probably at the naphthalic ring. Because the naphthalic ring is far away from the triphenylamino groups, the effect of the triphenylamino groups on the reduction potential is limited. The HOMO and LUMO energy

Table 2
Half-wave redox potentials[a] (vs. SCE) of compounds **2**–**4** in dried dichloromethane.

Compounds	Ox_3	Ox_2	Ox_1	Red_1	$E^{\theta}_{1/2}$ [b]	HOMO (eV)	LUMO (eV)
2			0.93	−1.35	2.28	−5.33	−3.05
3		0.87	0.51	−1.33	1.84	−4.91	−3.07
4	1.12	0.61	0.30	−1.26	1.56	−4.70	−3.14

[a] Values obtained by DPV in dry CH_2Cl_2 with 0.1 M TBAP as the supporting electrolyte and Fc/Fc^+ as internal standard.
[b] $E^{\theta}_{1/2} = E_{ox1} - E_{red1}$.

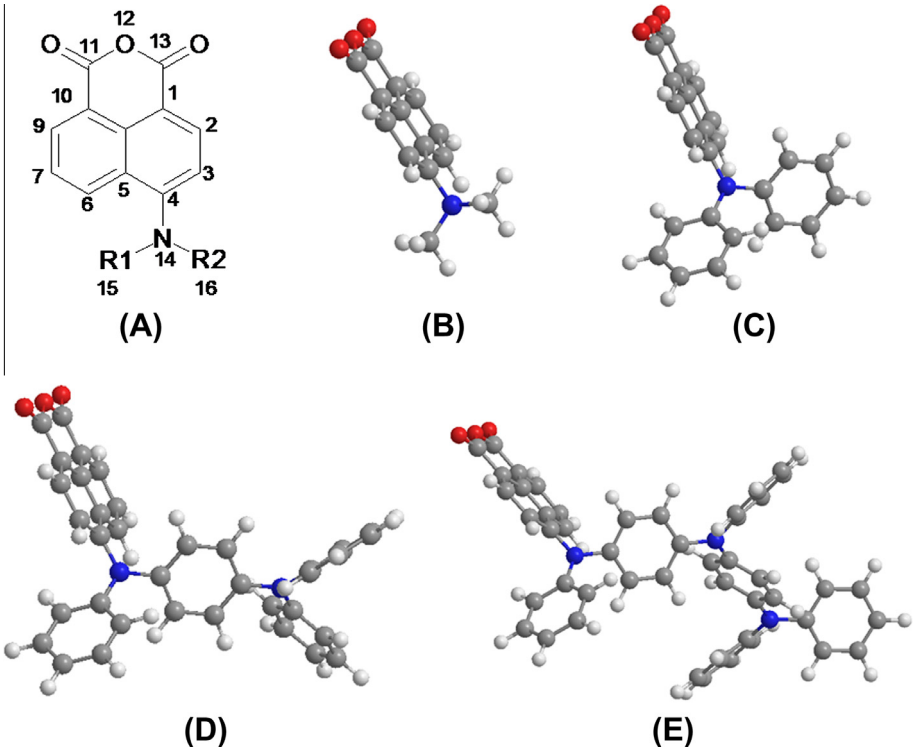

Fig. 3. Labels of the atoms in the molecular structure (A) during calculation and the minimized molecular structure of compounds **1**–**4** (B–E).

levels are also estimated from the oxidation potentials, the results are summarized in Table 2. It can be found that the energy of HOMO increases significantly from compounds **2** to **4**, which indicates that the introduction of electron donating groups varies the HOMO energy efficiently. However, the energy decrease of LUMO is very small, suggesting no large effect of the triphenylamino groups on LUMO energy. Due to the significant increase on the energy of HOMO along with the increase on the number of triphenylamino groups from compounds **2** to **4**, the energy gap between HOMO and LUMO decreases remarkably, and consequently the maximal absorption peak shifts to red dramatically.

3.5. Theoretical calculation

3.5.1. Minimized molecular structure

Using b3lyp/6-31g(d) method, the minimized structure of compounds **1**–**4** were optimized, Fig. 3. It is worth noting that similar calculating method has been used to calculate similar naphthalic anhydride compounds [24]. The resulted geometry and structure parameters are proved to be reliable by the crystal structure. Therefore, we choose the similar calculating method for our compounds. The calculated geometric parameters, including bond length and torsion angle are listed in Supporting Information. It can be seen that, naphthalic ring has a planar structure with a twisting angle of ~90° from the plane of directly connected amino group. The bonds which close to the C-4 positions of the naphthalic ring, including C4–N, N–R1, N–R2, C3–C4, C4–C5 are all get shorter a little bit when the side groups are introduced at C-4 positions, so as the angle of C4–N–R1, C4–N–R2. The bonds C3–C4 and C4–C5 were mostly impacted probably because of their adjacency with the substituents. The bond length of C3–C4 and C4–C5 in compound **1** is 1.403 and 1.450 Å, which decreased to 1.396 and 1.443 Å in compounds **2** and **3** and 1.398 and 1.444 Å in compound **4**. The bond length decrease of compounds **2**–**4** can be ascribed to the large steric hindrance introduced by the triphenylamino groups at the C-4 position. The bonds length of C4–N, N–R1 and N–R2 are also strongly affected by the substituents. Similar results can be found from the comparison of the bond length of C4–N, N–R1 and N–R2 in compounds **1**–**4**.

3.5.2. Calculated frontier molecular orbital

The distribution of frontier molecular orbitals as well as their energy levels is shown in Fig. 4. It can be found that the energy of the LUMOs is not significantly affected by the triphenylamino groups at C-4 position. The energies of LUMOs of compounds **1**–**4** are similar. But the energy of the HOMO increases dramatically along with the increase on the number of triphenylamino groups at C-4 position. The HOMO energy of compound **1** is −5.98 eV, which is significantly smaller than that of compound **4** (−4.86 eV). The result of this increase on the HOMO energy from compounds **1** to **4** is the decrease on the energy gap between HOMO and LUMO. The HOMO–LUMO energy gap decrease following the order of **1** > **2** > **3** > **4**, this is in line with the red shift on the ICT band in the UV–vis absorption spectra as shown in Fig. 1. This also suggests that the ICT transition is dominated by the transition from HOMO to LUMO in these compounds. It is notable that the calculated energies of HOMO and LUMO as shown Fig. 4are a little bit different from those measured by electrochemical method as shown in Table 2. This is because the quantum chemical calculation is performed on the molecules in vacuum while the electrochemical measurement is carried out on the molecules in solution. Nevertheless, the energies of HOMO and LUMO resulted from both quantum chemical calculation and electrochemical experiments change in the same trend along with

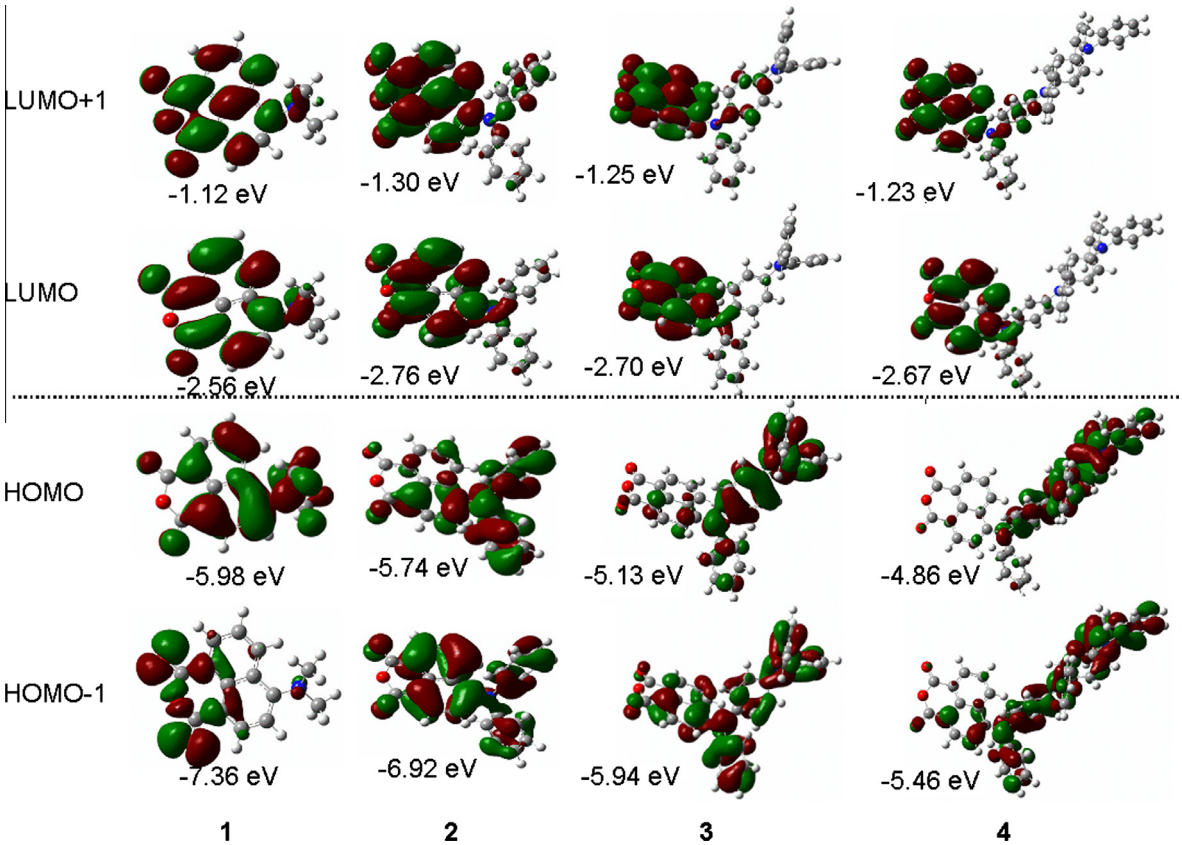

Fig. 4. Electronic density contours and the energy level of the frontier molecular orbitals for compounds **1**–**4**.

the increase on the number of triphenylamino groups, which indicates further that the results of quantum chemical calculation are reliable.

The distributions of the frontier molecular orbital on the molecular backbone illustrate visually the push–pull effects in these molecules. In the molecule of **1**, the HOMO distributes throughout the whole molecule, but with about 41.7% locates on the dimethylamino group. Meaning while, the LUMO spreads also over the molecule, with a contribution from dimethylamino group of only 7.9%. Transition from HOMO to LUMO under photoexcitation leads to charge redistribution over the whole molecule. A partial charge will move from dimethylamino group to the anhydride group along with this HOMO to LUMO transition. In compound **2**, the HOMO distributes mainly on the diphenylamine and the part of naphthalic ring close to the diphenylamine group. The contribution of the diphenylamine to the HOMO is about 71.1%. But the LUMO of compound **2** locates mainly on the naphthalic ring and the anhydride group. This indicates that the transition from HOMO to LUMO in compound **2** will leads to more significant charge transfer from electron donating diphenylamine group to naphthalic anhydride group than that happens in compound **1**. In compounds **3** and **4**, the HOMOs distribute almost 100% on the triphenylamino groups while the LUMOs are restricted on the naphthalic anhydride ring. Therefore, transition from HOMO to LUMO in these two compounds leads to an intramolecular electron transfer from the side group to the naphthalic anhydride ring instead of the ICT in compounds **1** and **2**. This is why the fluorescence of ICT, corresponding to HOMO–LUMO transition, in compounds **3** and **4** were completely quenched.

Besides the HOMO and LUMO, the distributions and energy levels of HOMO-1 are also shown in Fig. 4. The energy levels of HOMO-1 of these four compounds increase dramatically along with the increase on the number of triphenylamino groups at C-4 position. The HOMO-1 orbital in compound **1** located mainly on the anhydride groups, i.e. on the "pull" end. Along with the increase on the length of the electron donating side group, the HOMO-1 move gradually from the "pull" end to the "push" end. More than half of the electron cloudy of HOMO-1 of compound **3** distribute on the side group. The transition from HOMO-1 to LUMO in compound **3** will cause also a partial charge transfer as that induced by the transition from HOMO to LUMO in compounds **1** and **2**. Therefore, the emission band observed for compound **3** (at 562 nm) in Fig. 2 might be attributed in part to the excited state which is caused by the transition from HOMO-1 to LUMO. In compound **4**, however, the contribution of the side groups to HOMO-1 orbital increases to ~100%. Transition from HOMO-1 to LUMO in compound **4** will induce also an electron transfer from the triphenylamino groups to the naphthalic ring and then no emission from this excited state was observed.

4. Conclusion

In this paper we have designed and synthesized a series of "push–pull" naphthalic anhydride compounds with a linear triphenylamine oligomer of different length as electron donor. UV–vis absorption, emission spectra and theoretical calculation were revealed that with the increase on the number of triphenylamino groups at the "push" end, the red-shift on the absorption maximum and the energy gap between HOMO and LUMO decrease gradually. The decrease on the HOMO/LUMO energy gap is primarily caused by the increase on the energy level of HOMO. The fluorescence quantum yields of these compounds decrease also along with the increase on the number of triphenylamino groups at the "push" end due to the enhanced electron donating ability. The fluorescence quantum yields of compounds **3** and **4** are extremely small, which is because the process induced by photo excitation is no more ICT, but electron transfer from triphenylamines to naphthalic anhydride instead. More interestingly, compound **3** show a very weak emission at 560 nm after excitation at 440 nm. This weak emission might be assigned to a special ICT, which involve a high energy transition, such as the transition from HOMO-1 to LUMO. The results of this research revealed that for a "push–pull" molecule, strong electron donating ability at the "push" end could change the ICT into electron transfer and lead to a completely fluorescence quenching.

Acknowledgements

We thank the Natural Science Foundation of China (Grand Nos. 21073112 and 21173136), the National Basic Research Program of China (973 Program: 2012CB93280) and Natural Science foundation of Shandong Province (ZR2010EZ007) for the financial support.

Appendix A. Supplementary material

Supplementary data associated with this article can be found, in the online version, at http://dx.doi.org/10.1016/j.molstruc.2013.10.004.

References

[1] I. Grabchev, P. Meallier, T. Konstantmova, M. Popova, Dyes Pigm. 28 (1995) 41–46.
[2] J.X. Yang, X.L. Wang, T. Song, L.H. Xu, Dyes Pigm. 67 (2005) 27–33.
[3] S. Dhar, S.S. Roy, D.K. Rana, S. Bhattacharya, S.C. Bhattacharya, J. Phys. Chem. A 115 (2011) 2216–2224.
[4] Z. Cao, P. Nandhikonda, M.D. Heagy, J. Org. Chem. 74 (2009) 3544–3546.
[5] E.B. Veale, D.O. Frimannsson, M. Lawler, T. Gunnlaugsson, Org. Lett. 11 (2009) 4040–4043.
[6] I. Grabtchev, T. Philipova, Dyes Pigm. 27 (1995) 321–325.
[7] A.A. Fuller, F.J. Seidl, P.A. Bruno, M.A. Plescia, K.S. Palla, Pept. Sci. 96 (2011) 627–638.
[8] Z.C. Xu, X.H. Qian, J.N. Cui, Org. Lett. 7 (2005) 3029–3032.
[9] I. Grabchev, J.M. Chovelon, Polym. Degrad. Stabil. 92 (2007) 1911–1915.
[10] M. Kluciar, R. Ferreira, B. de Castro, U. Pischel, J. Org. Chem. 73 (2008) 6079–6085.
[11] H.S. Cao, D.I. Diaz, N.D. Cesare, J.R. Lakowicz, M.D. Heagy, Org. Lett. 4 (2002) 1503–1505.
[12] D. Srikun, E.W. Miller, D.W. Domaille, C.J. Chang, J. Am. Chem. Soc. 130 (2008) 4596–4597.
[13] E.B. Veale, T. Gunnlaugsson, J. Org. Chem. 73 (2008) 8073–8076.
[14] M. Dong, Y.W. Wang, Y. Peng, Org. Lett. 12 (2010) 5310–5313.
[15] W. Jiang, Y.M. Sun, X.L. Wang, Q. Wang, W.L. Xu, Dyes Pigm. 77 (2008) 125–128.
[16] A.D. Becke, Phys. Rev. A 38 (1988) 3098–3100.
[17] A.D. Becke, J. Chem. Phys. 98 (1993) 5648–5652.
[18] M.D. Halls, J. Velkovski, H.B. Schlegel, Theor. Chem. Acc. 150 (2001) 413–421.
[19] K.K. Ong, J.O. Jensen, H.F. Hameka, J. Mol. Struct. (Theochem) 459 (1999) 131–144.
[20] A.Y. Kobitski, R. Scholz, D.R.T. Zahn, J. Mol. Struct. (Theochem) 625 (2003) 39–46.
[21] A.E. Reed, L.A. Curtiss, F. Weinhold, Chem. Rev. 88 (1988) 899–926.
[22] M.J. Frisch, G.W. Trucks, H.B. Schlegel, G.E. Scuseria, M.A. Robb, J.R. Cheeseman, J.A. Montgomery, Jr., T. Vreven, K.N. Kudin, J.C. Burant, J.M. Millam, S.S. Iyengar, J. Tomasi, V. Barone, B. Mennucci, M. Cossi, G. Scalmani, N. Rega, G.A. Petersson, H. Nakatsuji, M. Hada, M. Ehara, K. Toyota, R. Fukuda, J. Hasegawa, M. Ishida, T. Nakajima, Y. Honda, O. Kitao, H. Nakai, M. Klene, X. Li, J.E. Knox, H.P. Hratchian, J.B. Cross, C. Adamo, J. Jaramillo, R. Gomperts, R.E. Stratmann, O. Yazyev, A.J. Austin, R. Cammi, C. Pomelli, J.W. Ochterski, P.Y. Ayala, K. Morokuma, G.A. Voth, P. Salvador, J.J. Dannenberg, V.G. Zakrzewski, S. Dapprich, A.D. Daniels, M.C. Strain, O. Farkas, D.K. Malick, A.D. Rabuck, K. Raghavachari, J.B. Foresman, J.V. Ortiz, Q. Cui, A.G. Baboul, S. Clifford, J. Cioslowski, B.B. Stefanov, G. Liu, A. Liashenko, P. Piskorz, I. Komaromi, R.L. Martin, D.J. Fox, T. Keith, M.A. Al-Laham, C.Y. Peng, A. Nanayakkara, M. Challacombe, P.M. W. Gill, B. Johnson, W. Chen, M.W. Wong, C. Gonzalez, J.A. Pople, Gaussian 03, Revision B.05; Gaussian, Inc., Pittsburgh, PA, 2003.
[23] J. Kollár, P. Hrdlovic, Š. Chmelaa, M. Sarakhab, G. Guyot, J. Photochem. Photobiol. A: Chem. 170 (2005) 151–159.

[24] A. Islam, C.C. Cheng, S.H. Chi, P.G. Hela, I.C. Chen, C.H. Cheng, J. Phys. Chem. B 109 (2005) 5509–5517.
[25] F. D'Souza, S. Gadde, D.M.S. Islam, C.A. Wijesinghe, A.L. Schumacher, M.E. Zandler, Y. Araki, O. Ito, J. Phys. Chem. A 111 (2007) 8552–8560.
[26] D.F. Cauble, V. Lynch, M.J. Krische, J. Org. Chem. 68 (2003) 15–21.
[27] D.W. Cho, M. Fujitsuka, A. Sugimoto, T. Majima, J. Phys. Chem. A 112 (2008). 7208-7203.
[28] R. Ferreira, C. Baleizão, J.M. Muñoz-Molina, M.N. Berberan-Santos, U. Pischel, J. Phys. Chem. A 115 (2011) 1092–1099.
[29] J.X. Yang, X.L. Wang, X.M. Wang, L.H. Xu, Dyes Pigm. 66 (2005) 83–87.